

I; those with angiographic risks as Grade II; those with medical risks as Grade III; and those with neurological risks as Grade IV. This grading scale classifies patients with CA stenosis regardless of their clinical presentation, whether symptomatic or asymptomatic. Those in Grade IV were neurologically unstable at the time of CEA. Therefore, Grade IV patients were a subgroup of symptomatic patients.

Echolucent plaques have been suggested to possess a higher embolic potential when treated using CAS.⁵ We previously described the outcome of CEA and CAS in prospectively classified patients by using the Sundt CEA risk classification system. A higher incidence of neurological morbidity and more lesions were noted on diffusion weighted MR images after CAS in Grades II and III patients combined than in Grade I patients.¹⁷ We can speculate on the high prevalence of unstable plaques with higher embolic potential in Grades II and III patients than in Grade I patients. So far, morphological observation of CA plaques in patients, classified into symptomatic and asymptomatic groups, has been presented.^{4,9,14-16,18,22,23,27} However, there are no precise reports on the histopathological features of endarterectomy specimens in patients with primary CA stenosis, correlated with the CEA risk classification system. In the present report, we determined the pathological features of CA plaques in patients classified according to this risk grading scale. Furthermore, we examined whether the plaque with high embolic potential after CA intervention, particularly CAS, could be predicted based on clinical risks for CEA.

Methods

Carotid Endarterectomy Specimens and Classification of Patients

We selected 85 plaques in 82 patients (75 men and 7 women) with a mean age of 69.0 ± 6.7 years who underwent CEA for primary CA stenosis at the National Cerebral and Cardiovascular Center, Suita, Japan, between 2000 and 2005. A CEA was considered the first line of therapy; CAS was indicated mainly in high-risk patients, including those who were ineligible for CEA by the North American Symptomatic Carotid Endarterectomy Trial (NASCENT),¹ those with echogenic plaques, and those who expressed a preference for the CAS procedure. These patients were prospectively registered and classified into 4 groups: those without angiographic, medical, and neurological risks (Grade I, 27 cases); those with angiographic risk but without medical and neurological risks (Grade II, 10 cases); those with medical risk but without neurological risk (Grade III, 31 cases); and those with neurological risk (Grade IV, 17 cases). The number of plaques in Grade II patients was too small for statistical analysis; therefore, we excluded these patients from the present investigation. The patients were also classified as either symptomatic or asymptomatic based on their medical history. Symptomatic patients had experienced a transient ischemic attack, stroke, or amaurosis fugax. The degree of CA stenosis was measured on digital subtraction angiography, and the indications for intervention were as follows: for symptom-

atic cases, 70% or greater stenosis; and for asymptomatic cases, 75% or greater stenosis. We examined 75 plaques; lesions caused symptoms in 52 plaques (69.3%). Factors that were regarded as an angiographic risk included occlusion of the opposite internal CA, stenosis of the internal CA in the region of the carotid siphon, extension of the plaque greater than 5 cm proximally in the common CA, bifurcation of the CA at C-2 in conjunction with a short, thick neck, evidence of a thrombus extending from an ulcerative lesions, and carotid slim sign. Angina pectoris, a recent myocardial infarction within 6 months prior to the CEA, congestive heart failure, severe hypertension (blood pressure > 180/110 mm Hg), advanced peripheral arterial occlusive disease, and age older than 75 years were considered to represent medical risk. Progressing neurological deficit, recently resolved neurological deficit within 24 hours prior to CEA, generalized cerebral ischemia, a recent cerebral infarction within 7 days prior to the date of surgery, and frequent transient ischemic attacks not controlled by anticoagulants were regarded as neurological risks.

Light Microscopy and Analysis of Pathological Features

Surgically removed CA plaques were fixed in 20% buffered formalin and decalcified with EDTA. The specimens were embedded in paraffin, and transverse sections were cut at 5-mm intervals over the entire length. Fragmented plaques were excluded from the study. Luminal narrowing was defined as the ratio of lumen area/removed vessel area and was measured using an image analysis system equipped with a digital camera (Microscope System DP71, Olympus Co.) and software (WinROOF, Mitani Corp.). Microscopic sections, stained with H & E and Masson trichrome, were used for analysis of overall morphology, thickness of the fibrous cap, definition of plaque disruption, healed plaque rupture, and thrombosis. Plaque rupture or ulceration resulted in exposure of cholesterol crystals, necrotic debris, or lipid-laden macrophages to the lumen surface. When the fibrous cap exhibited disruption with layers of immature collagen, accompanied by proliferation of capillaries, it was considered to have undergone plaque rupture. Healed rupture was examined by Masson trichrome stain (healed sites are indicated by the light blue color) and by picosirius red staining followed by polarization microscopy.⁶ The same approach was used in cases with a multilayered fibrous cap, multiple necrotic cores, and fibrin deposition into the necrotic core. The length of the IEL was calculated from sections stained with Elastica van Gieson. Light microscopy evaluation was performed by 2 independent investigators (H.H. and H.I.U.) who were blinded to the clinical status of the patients.

Immunohistochemical and Morphometric Analysis

The primary antibodies used were mouse monoclonal antibodies against CD68 (working dilution 1:100, Dako), glycophorin A (working dilution 1:50, Dako), and adipophilin (working dilution 1:200, American Research Products). Heat-induced epitope retrieval was always performed. Mouse IgG1 (Dako) was used in equivalent

dilutions as a negative control. Using the image analysis system and the software mentioned above, we measured the glycoprotein A-positive area and defined the ratio glycoprotein A-positive area/vessel area for quantification of IPH. We also measured CD68- and adipophilin-positive areas and calculated the following ratios: the CD68-positive area/vessel area, the CD68-positive area in the fibrous cap/fibrous cap area, the adipophilin-positive area/vessel area, and the adipophilin-positive area/CD68-positive area.

Statistical Analysis

Results are presented as the means \pm SEMs for continuous variables. For statistical analysis, differences between groups were evaluated using the chi-square or Fisher exact test (for categorical variables) and the t-test (for continuous variables). Two-sided p values < 0.05 were considered significant.

Results

We analyzed 75 CA plaques obtained from 72 patients. There were 27 plaques in Grade I, 31 in Grade III, and 17 in Grade IV patients. The mean CA luminal narrowing and the length of the IEL in Grades I, III, and IV patients were similar. The percentage of the necrotic core area gradually increased as the risk of CEA increased, but no statistical difference was observed among these

3 groups. The calcified area/total vessel area and the CD68-positive macrophage area/total vessel area ratios also showed no significant difference among the groups. However, the CD68-positive cells occupied a significantly larger area of the fibrous cap in plaques in Grade IV patients than those in Grades I and III patients (Table 1).

The mean thickness of the fibrous cap obtained from plaques in Grades I, III, and IV patients measured 423.0 ± 93.8 , 91.9 ± 10.9 , and 46.6 ± 10.4 μm , respectively. A significantly thicker fibrous cap was observed in plaques in Grade I patients. The degree of IPH, as determined by the glycoprotein A-positive area/vessel area, was significantly larger in plaques in Grades III and IV patients than those in Grade I patients (Fig. 1 and Table 1). Plaque disruption was more frequently identified in Grade IV than in Grades I and III patients (Fig. 2 and Table 1). Some of the disrupted plaques (27.8%) showed low-grade stenosis, which demonstrated less than 75% of stenosis of the vessel area (Fig. 3), whereas the frequency of plaque disruption in low-grade stenosis was similar in each grade (data not shown).

Healed plaque rupture was detected equally among groups at incidences of 70.0%, 74.2%, and 70.6% in plaques in Grades I, III, and IV patients, respectively. Histological features of a multilayered fibrous cap were frequently present in the higher CEA risk group, but a statistically significant difference was not detected (Table 1 and Fig. 4). Fresh thrombi were more frequent in Grade IV patients than in Grade I patients (Table 1).

TABLE 1: Pathological features of CA plaques in patients classified according to the CEA risk classification system

Characteristic	Grade		
	Neurologically Stable		Neurologically Unstable
	I (27 cases)	III (31 cases)	IV (17 cases)
mean \pm SEM			
age (yrs)	67.5 \pm 0.9	70.0 \pm 1.6	71.0 \pm 1.5
area of stenosis (%)	86.6 \pm 2.0	91.6 \pm 1.5	82.5 \pm 2.1
length of IEL (mm)	24.2 \pm 1.2	24.9 \pm 1.0	26.4 \pm 2.1
fibrous cap thickness (μm)	423.0 \pm 93.8*†	91.9 \pm 10.9†	46.6 \pm 10.4
no. of cases (%)			
plaque disruption	8 (29.6)†	14 (45.2)‡	14 (82.4)
multilayered fibrous cap	12 (44.4)	16 (51.6)	12 (70.6)
fresh thrombus	1 (3.7)‡	2 (6.5)	5 (29.4)
organized thrombus	8 (29.6)‡	13 (41.9)	11 (64.7)
ratio (mean \pm SEM; %)			
necrotic core/vessel area	29.5 \pm 4.7	34.4 \pm 3.8	37.5 \pm 6.7
glycoprotein A/vessel area	4.5 \pm 1.0‡,§	10.1 \pm 1.9	8.4 \pm 1.1
calcification/vessel area	5.8 \pm 2.9	3.2 \pm 1.3	6.3 \pm 3.5
CD68/vessel area	4.2 \pm 0.5	3.7 \pm 0.5	3.8 \pm 0.5
CD68/cap area	2.5 \pm 0.5‡	3.0 \pm 0.7‡	5.1 \pm 0.8
adipophilin/vessel area	1.3 \pm 0.3‡	1.2 \pm 0.3‡	2.2 \pm 0.4
adipophilin/CD68 area	26.4 \pm 3.7†	32.8 \pm 5.5‡	55.6 \pm 6.5

* p < 0.005 , versus Grade III.

† p < 0.005 , versus Grade IV.

‡ p < 0.05 , versus Grade IV.

§ p < 0.05 , versus Grade III.

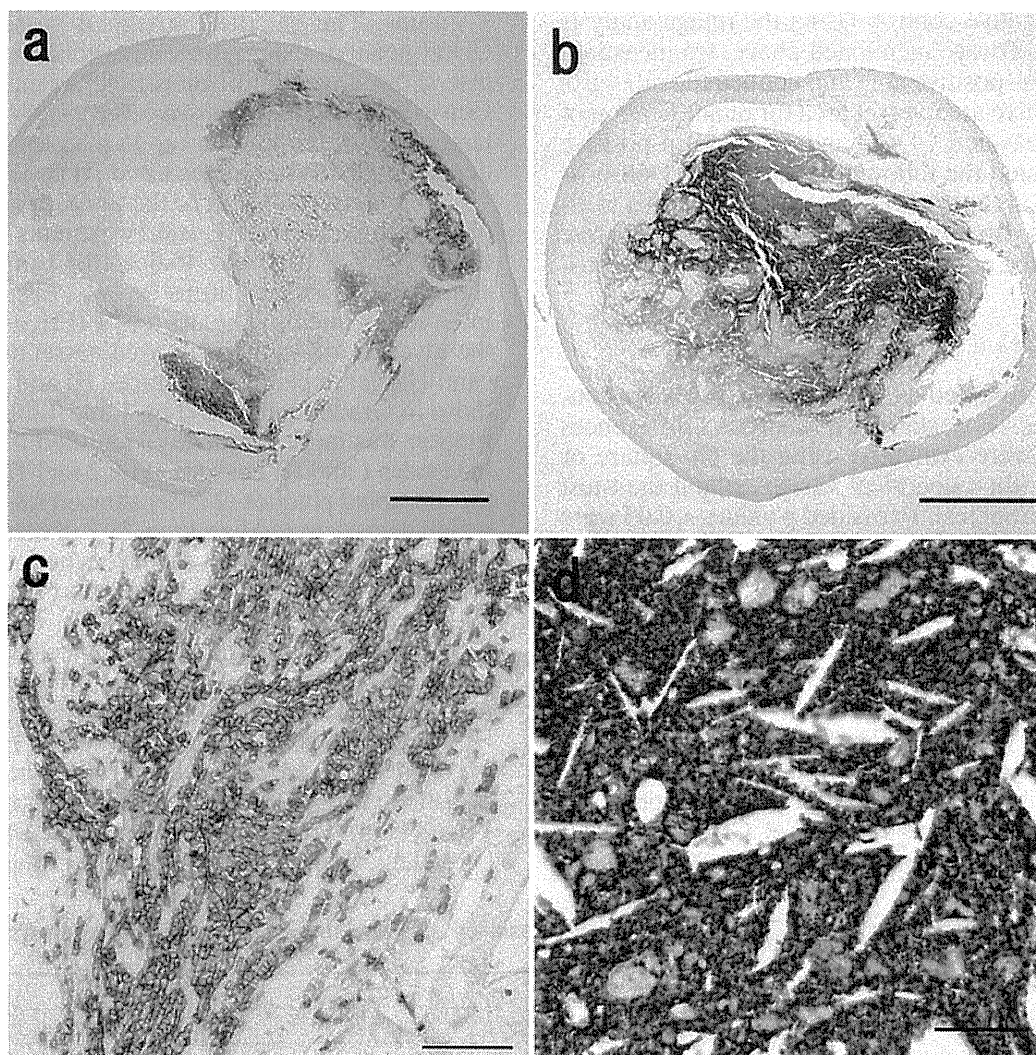


FIG. 1. Photomicrographs showing the different degree of immunohistochemistry of glycoprotein A, demonstrating fresh and recent IPH of CA plaques. The *brown areas* indicate positive staining of glycoprotein A. **a and b:** Morphometric analysis showing 13.3% (**a**) and 36.3% (**b**) of glycoprotein A-positive area/total vessel area, respectively. **c and d:** Higher magnification of the positive staining of glycoprotein A in erythrocyte membranes (**c**) and its remnants (**d**) at the necrotic core area of the CA. Scale bar = 2 mm (**a and b**); 50 μ m (**c and d**).

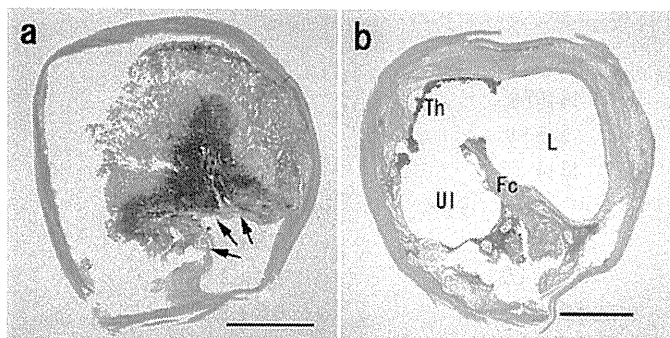


FIG. 2. Photomicrographs of plaque rupture (**a**) and ulceration (**b**) of carotid atherosclerotic lesions. **a:** The fibrous cap has burst into the necrotic core (*arrows*), which is a less common feature in a rupture of a coronary artery plaque, indicating high blood flow of the CA. **b:** Ulceration is identified by crater formation induced by the previous plaque rupture with mural thrombus formation (Th) in a cast-off shell of plaque and true lumen. The true vessel lumen (L) is connected to the ulcerated plaque area (UI). Between the vessel lumen and ulcer, there is a remnant of ruptured fibrous cap (Fc). Masson trichrome, scale bar = 2 mm.

Adipophilin was often present near the necrotic regions of plaques, especially at the fibrous cap and shoulder regions of the plaque. Adipophilin-positive cells were noted to be CD68-positive macrophages by serial sections (Fig. 5). The ratio of adipophilin-positive area/vessel area and adipophilin-positive area/CD68-positive area were larger in Grade IV patients than in Grades I and III patients (Table 1).

We also compared the histological features of symptomatic patients in Grades I and III with those of asymptomatic patients in those grades. In Grades I and III patients, 15 (55.6%) and 20 (64.5%) cases, respectively, were symptomatic. Regardless of presentation, histological features of CA plaques were similar between symptomatic and asymptomatic subgroups in Grades I and III patients (Table 2). All of the Grade IV patients were symptomatic.

Discussion

The CEA risk classification system, established by

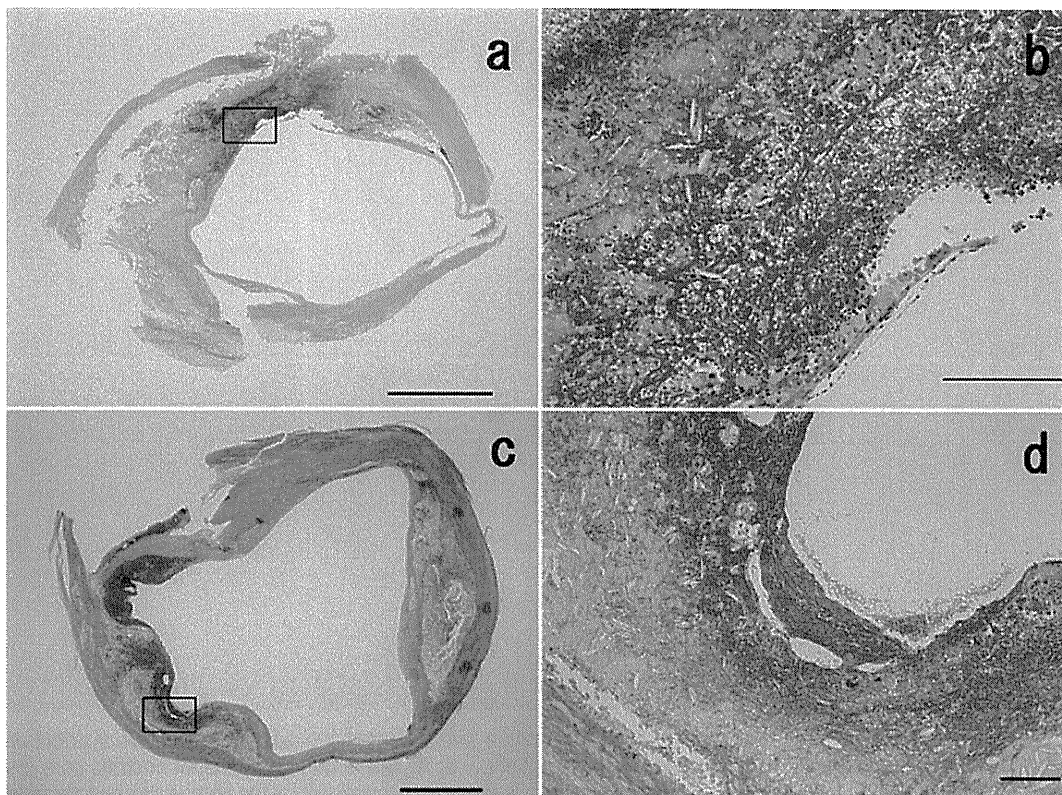


Fig. 3. Photomicrographs of atherosclerotic CA plaques demonstrating vulnerable (**a and b**) and disrupted (**c and d**) plaques with mild to moderate narrowing of the lumen with IPH. **a and c:** Image analysis systems introduce an area stenosis of 67.2% (**a**) and 53.3% (**c**). **b and d:** High-magnification views taken from the boxed area in panels **a** and **c**. A thin fibrous cap accompanied by foam cell infiltration (**b**) and a disrupted fibrous cap with superimposed mural thrombi (**d**) are seen. Both cases complicate massive IPH with fibrin deposition in necrotic core. Masson trichrome, scale bar = 2 mm (**a and c**); 200 μ m (**b and d**).

Sundt and colleagues,³⁰ is widely accepted to evaluate patients with CA stenosis. This retrospective analysis of patients in the 1970s served as a prospective classification for patients undergoing CEA.³¹ Recently, based on this grading scale, we prospectively compared perioperative neurological morbidity and ischemia in patients who underwent CEA or CAS by examining MR imaging findings.¹⁷ Higher rates of morbidity and increased lesions after CAS than after CEA were identified on diffusion weighted images. A higher incidence of neurological deficits and new lesions on MR images after CAS occurred among patients with angiographic and medical risks (Grades II and III) than among those without any risks (Grade I). Furthermore, echolucent plaques have been described to have a significantly higher embolic potential when treated with CAS.⁵ Therefore, precise knowledge of the histopathology of CA plaques in different clinical risk groups is important to select the method of vascular intervention and predict eventual complications.

The present study demonstrated that plaques in Grade III patients were similar to those in Grade IV patients in that they both had a thin fibrous cap with an enhanced degree of IPH. These results suggest a role of IPH in plaque progression, and they support the clinical evidence of a higher incidence of lesions assessed using MR imaging after CAS in Grades II and III patients than in Grade I patients.¹⁷ A subgroup analysis of Grades I and III patients based on case presentation identified no significant difference between symptomatic and asymptomatic pa-

tients in each group (Table 2), although there seemed to be a tendency for a higher frequency of plaque disruption and organized thrombus formation in symptomatic than in asymptomatic Grade III patients. The lack of statistical significance is possibly dependent on the limited number of cases for these histological parameters. This result indicates that distinct histological features in plaques in Grade III compared with Grade I patients are correlated

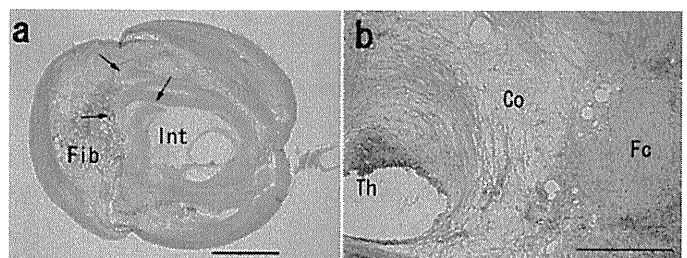


Fig. 4. **a:** Representative photomicrograph of a multilayered fibrous cap with multiple necrotic cores and fibrin deposition inside the core. The piled-up fibrous caps partially break (*arrow*) and multiple necrotic cores with fibrin deposition (Fib) are identified. The intima (Int) of the luminal portion is composed of immature connective tissue (*light blue*), and these histological features indicate repeated plaque rupture and healing processes. **b:** A photomicrograph of a healed rupture showing a layer of immature collagen (Co) overlying the fibrous cap with proliferation of capillaries. The thrombus is recognized at the surface of narrowing vessel lumen. Masson trichrome, scale bar = 2 mm (**a**); 500 μ m (**b**).

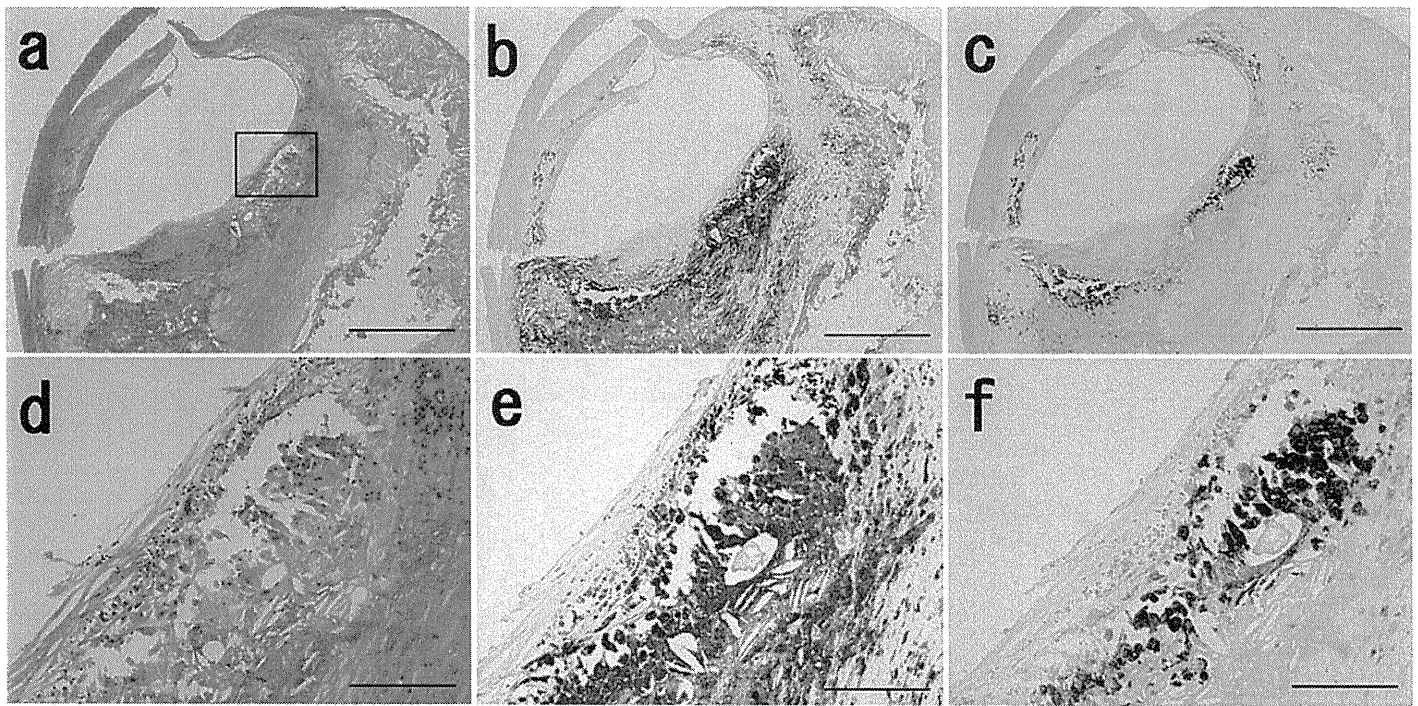


FIG. 5. Photomicrographs showing dense macrophage infiltration and its enhanced adipophilin protein distribution at the fibrous cap of plaque obtained from a neurologically unstable patient. **a:** A plaque with an abundant necrotic core and a thin fibrous cap. **b:** CD68-positive macrophages infiltrate abundantly in the plaque, especially at the fibrous cap and shoulder lesion of plaque by immunohistochemical analysis. **c:** Serial section of panel **b** showing that adipophilin-positive cells are CD68-positive macrophages. The distribution of adipophilin is located predominantly at the thin fibrous cap. **d–f:** High-magnification views of panels **a–c**, corresponding to the boxed area in panel **a**. H & E (**a and d**), CD68 (**b and e**), adipophilin (**c and f**). Scale bar = 1 mm (**a–c**); 200 μ m (**d–f**).

TABLE 2: Histological features based on case presentation in Grades I and III patients

Characteristic	Grade I		p Value	Grade III		p Value
	Symptomatic (15 cases)	Asymptomatic (12 cases)		Symptomatic (20 cases)	Asymptomatic (11 cases)	
mean \pm SEM						
age (yrs)	66.9 \pm 0.8	68.3 \pm 1.8	0.471	70.1 \pm 1.9	69.9 \pm 2.9	0.967
area stenosis (%)	85.9 \pm 2.9	87.4 \pm 3.2	0.713	91.0 \pm 1.9	92.7 \pm 2.3	0.553
length of IEL (mm)	24.8 \pm 1.5	23.5 \pm 2.0	0.588	25.8 \pm 1.3	23.2 \pm 1.5	0.181
fibrous cap thickness (mm)	480.3 \pm 134.1	351.2 \pm 138.1	0.492	82.0 \pm 10.9	110.0 \pm 22.5	0.261
no. of cases (%)						
plaque disruption	4 (26.7)	4 (33.3)	0.516	11 (55.0)	3 (27.3)	0.134
multilayered fibrous cap	5 (33.3)	7 (58.3)	0.363	9 (45.0)	7 (63.6)	0.537
fresh thrombus	0 (0)	1 (8.3)	0.464	2 (10.0)	0 (0)	0.409
organized thrombus	4 (26.7)	4 (33.3)	0.516	10 (50.0)	3 (27.3)	0.200
ratio (mean \pm SEM; %)						
necrotic core/vessel area	23.1 \pm 6.1	37.4 \pm 7.2	0.130	35.1 \pm 5.1	33.3 \pm 7.0	0.829
glycophorin A/vessel area	2.9 \pm 0.9	6.4 \pm 2.0	0.123	9.8 \pm 2.3	10.8 \pm 3.6	0.796
calcification/vessel area	6.9 \pm 4.3	4.4 \pm 4.1	0.673	2.0 \pm 1.0	5.5 \pm 3.2	0.290
CD68/vessel area	3.5 \pm 0.8	5.1 \pm 0.8	0.147	3.7 \pm 0.6	3.8 \pm 1.1	0.985
CD68/cap area	2.1 \pm 0.7	2.9 \pm 0.9	0.465	2.6 \pm 0.7	3.6 \pm 1.4	0.527
adipophilin/vessel area	1.0 \pm 0.2	1.6 \pm 0.6	0.249	1.2 \pm 0.3	1.3 \pm 0.5	0.779
adipophilin/CD68 area	25.3 \pm 4.6	27.9 \pm 6.5	0.738	32.2 \pm 6.7	34.0 \pm 9.9	0.879

with the CEA risk classification system, regardless of clinical presentation.

Atherosclerosis is considered to be a generalized disease, and an association between CA atherosclerosis and coronary artery disease has been well established. It is well known that prevalence of CA stenosis is high in patients with coronary artery diseases.^{25,32} Complication of medical risks for Grade III patients, such as angina pectoris or a recent myocardial infarction, indicates the presence of a progressive atherosclerotic lesion in their coronary artery tree. Therefore, it is logical that unstable CA plaques showing thin fibrous cap and enhanced IPH were prevalent in patients with medical risks.

Our clinical¹⁷ and histopathological observation of CA plaques based on the CEA risk classification system and previous studies concerning CA pathology and morphology^{5,9,13,15,16,19,27,33,35} indicated that CAS in Grades III and IV patients needs a preliminary careful evaluation of plaque characteristics. In light of the present histological study combined with the reported higher complication rates of CAS for patients with vascular and medical risk profiles, CA imaging to detect plaques with high embolic potential is important for optimal triage of patients with CA stenosis. Among noninvasive plaque imaging, MR imaging techniques have been used in CA plaque characterization and are highly sensitive and specific in resolving lipid-rich necrotic core regions, IPH, and fibrous cap thickness.^{7,8,10,20,36} Thus, MR imaging may be a useful application to detect a thin fibrous cap with an enhanced degree of IPH. Along with the results of the current study, we propose the following morphological criteria for CAS indication: a fibrous cap more than 300 μm thick, a necrotic core area/vessel area less than 30%, an IPH area/vessel area less than 5%, and an absence of plaque disruption. In cases of a thin fibrous cap atheroma with prominent IPH, CAS should be avoided, and CEA should be selected as the treatment modality.

This is the first report that has demonstrated a high degree of adipophilin expression in macrophages in the fibrous cap of CA plaques obtained from Grade IV patients. A recent study demonstrated increased adipophilin expression in symptomatic compared with asymptomatic CA plaques by real-time reverse transcription polymerase chain reaction and western blot analysis. Adipophilin expression was associated with red blood cells and cholesterol crystals,²⁴ but a precise correlation between adipophilin distribution and risk grading was not shown. It is known that adipophilin expression is enhanced by oxidized low-density lipoprotein;³⁴ when expressed, adipophilin enhances lipid accumulation and prevents lipid efflux from foam cells.²¹ This may in turn enhance inflammatory phenomena in the fibrous cap and thus induce plaque vulnerability.

Wasserman et al.³⁵ reported evidence of unstable plaques with low-grade CA stenosis by using MR imaging, whereas there is no description concerning the frequency of plaque disruption with low-grade CA stenosis, confirmed by histology. In this study, about 25% of CA plaque disruption corresponded to low-grade stenosis. This result suggested that the culprit lesion does not always correspond to a severe stenotic lesion, and it also emphasized that examination of the plaque component is

more important compared with the degree of stenosis in CA plaques. Blood flow is significantly higher in the CA than in the coronary artery, and this may cause ulceration and rupture even in cases of low-grade stenosis. Histological evidence of healed rupture was more frequently detected in CA plaques in our study than in the coronary artery with sudden coronary death.⁶ In addition, approximately one-half of our cases had a multilayered fibrous cap, while such change is less common in the coronary artery tree. A high incidence of healed rupture and observation of a multilayered fibrous cap suggest that repeated plaque rupture followed by healing processes may play an important role for progression of CA plaque.

Conclusions

We have shown that CA plaque in Grades III and IV patients is characterized by thinning of the fibrous cap and enhanced IPH. Adipophilin expression by macrophages in the fibrous cap appears to be correlated with neurological risks for CEA. Grades III and IV patients may have a higher risk of CAS complications; in these patients, maximum efforts should be made to characterize the plaque morphology by plaque imaging, such as MR imaging before CA intervention. In CA plaques demonstrating a thin fibrous cap and IPH, the CAS procedure should be avoided and CEA should instead be performed.

Disclosure

This work was funded in part by Grant-in-Aid for Researchers, Hyogo College of Medicine, 2007.

Author contributions to the study and manuscript preparation include the following. Conception and design: Hao, Iihara, Saito, Hirota. Acquisition of data: Hao, Ishibashi-Ueda. Analysis and interpretation of data: Hao, Iihara, Ishibashi-Ueda. Drafting the article: Hao. Critically revising the article: Iihara, Ishibashi-Ueda, Saito. Reviewed final version of the manuscript and approved it for submission: all authors. Statistical analysis: Hao. Administrative/technical/material support: Iihara. Study supervision: Saito, Hirota.

Acknowledgments

The authors thank Dr. Guillaume J. van Eys (Department of Genetics and Cell Biology, Cardiovascular Institute Maastrich, University of Maastrich, The Netherlands), and Dr. Giulio Gabbiani (Department of Pathology and Immunology, University of Geneva-CMU, Geneva, Switzerland) for their critical reading of the manuscript and helpful comments. They also thank Nobuyoshi Imai and Ryoji Hariyama for their technical assistance. Dr. Saito died after submission of this manuscript.

References

1. Anonymous: Beneficial effect of carotid endarterectomy in symptomatic patients with high-grade carotid stenosis. North American Symptomatic Carotid Endarterectomy Trial Collaborators. *N Engl J Med* **325**:445–453, 1991
2. Anonymous: Endarterectomy for asymptomatic carotid artery stenosis. Executive Committee for the Asymptomatic Carotid Atherosclerosis Study. *JAMA* **273**:1421–1428, 1995
3. Anonymous: Randomised trial of endarterectomy for recently symptomatic carotid stenosis: final results of the MRC European Carotid Surgery Trial (ECST). *Lancet* **351**:1379–1387, 1998
4. Bassiouny HS, Davis H, Massawa N, Gewertz BL, Glagov

- S, Zarins CK: Critical carotid stenoses: morphologic and chemical similarity between symptomatic and asymptomatic plaques. **J Vasc Surg** 9:202–212, 1989
5. Biasi GM, Froio A, Diethrich EB, Deleo G, Galimberti S, Mingazzini P, et al: Carotid plaque echolucency increases the risk of stroke in carotid stenting: the Imaging in Carotid Angioplasty and Risk of Stroke (ICAROS) study. **Circulation** 110:756–762, 2004
 6. Burke AP, Kolodgie FD, Farb A, Weber DK, Malcom GT, Smialek J, et al: Healed plaque ruptures and sudden coronary death: evidence that subclinical rupture has a role in plaque progression. **Circulation** 103:934–940, 2001
 7. Cai J, Hatsukami TS, Ferguson MS, Kerwin WS, Saam T, Chu B, et al: In vivo quantitative measurement of intact fibrous cap and lipid-rich necrotic core size in atherosclerotic carotid plaque: comparison of high-resolution, contrast-enhanced magnetic resonance imaging and histology. **Circulation** 112:3437–3444, 2005
 8. Cai JM, Hatsukami TS, Ferguson MS, Small R, Polissar NL, Yuan C: Classification of human carotid atherosclerotic lesions with in vivo multicontrast magnetic resonance imaging. **Circulation** 106:1368–1373, 2002
 9. Carr S, Farb A, Pearce WH, Virmani R, Yao JS: Atherosclerotic plaque rupture in symptomatic carotid artery stenosis. **J Vasc Surg** 23:755–766, 1996
 10. Chu B, Kampschulte A, Ferguson MS, Kerwin WS, Yarnykh VL, O'Brien KD, et al: Hemorrhage in the atherosclerotic carotid plaque: a high-resolution MRI study. **Stroke** 35:1079–1084, 2004
 11. Cunningham EJ, Bond R, Mehta Z, Mayberg MR, Warlow CP, Rothwell PM: Long-term durability of carotid endarterectomy for symptomatic stenosis and risk factors for late postoperative stroke. **Stroke** 33:2658–2663, 2002
 12. Eliasziw M, Streifler JY, Fox AJ, Hachinski VC, Ferguson GG, Barnett HJ: Significance of plaque ulceration in symptomatic patients with high-grade carotid stenosis. North American Symptomatic Carotid Endarterectomy Trial. **Stroke** 25:304–308, 1994
 13. Fischer U, Arnold M, Nedeltchev K, Brekenfeld C, Ballinari P, Remonda L, et al: NIHSS score and arteriographic findings in acute ischemic stroke. **Stroke** 36:2121–2125, 2005
 14. Fisher M, Paganini-Hill A, Martin A, Cosgrove M, Toole JF, Barnett HJ, et al: Carotid plaque pathology: thrombosis, ulceration, and stroke pathogenesis. **Stroke** 36:253–257, 2005 [Erratum in **Stroke** 36:2330, 2005]
 15. Gao P, Chen ZQ, Bao YH, Jiao LQ, Ling F: Correlation between carotid intraplaque hemorrhage and clinical symptoms: systematic review of observational studies. **Stroke** 38:2382–2390, 2007
 16. Golledge J, Greenhalgh RM, Davies AH: The symptomatic carotid plaque. **Stroke** 31:774–781, 2000
 17. Iihara K, Murao K, Sakai N, Yamada N, Nagata I, Miyamoto S: Outcome of carotid endarterectomy and stent insertion based on grading of carotid endarterectomy risk: a 7-year prospective study. **J Neurosurg** 105:546–554, 2006
 18. Imparato AM, Riles TS, Mintzer R, Baumann FG: The importance of hemorrhage in the relationship between gross morphologic characteristics and cerebral symptoms in 376 carotid artery plaques. **Ann Surg** 197:195–203, 1983
 19. Jander S, Sitzer M, Schumann R, Schroeter M, Siebler M, Steinmetz H, et al: Inflammation in high-grade carotid stenosis: a possible role for macrophages and T cells in plaque destabilization. **Stroke** 29:1625–1630, 1998
 20. Kampschulte A, Ferguson MS, Kerwin WS, Polissar NL, Chu B, Saam T, et al: Differentiation of intraplaque versus juxtalumenal hemorrhage/thrombus in advanced human carotid atherosclerotic lesions by in vivo magnetic resonance imaging. **Circulation** 110:3239–3244, 2004
 21. Larigauderie G, Bouhlef MA, Furman C, Jaye M, Fruchart JC, Rouis M: Perilipin, a potential substitute for adipophilin in triglyceride storage in human macrophages. **Atherosclerosis** 189:142–148, 2006
 22. Lennihan L, Kupsky WJ, Mohr JP, Hauser WA, Correll JW, Quest DO: Lack of association between carotid plaque hematoma and ischemic cerebral symptoms. **Stroke** 18:879–881, 1987
 23. Milei J, Parodi JC, Ferreira M, Barrone A, Grana DR, Maturri L: Atherosclerotic plaque rupture and intraplaque hemorrhage do not correlate with symptoms in carotid artery stenosis. **J Vasc Surg** 38:1241–1247, 2003
 24. Nuotio K, Isoviita PM, Saksi J, Ijäs P, Pitkaniemi J, Sonninen R, et al: Adipophilin expression is increased in symptomatic carotid atherosclerosis: correlation with red blood cells and cholesterol crystals. **Stroke** 38:1791–1798, 2007
 25. O'Leary DH, Polak JF, Kronmal RA, Kittner SJ, Bond MG, Wolfson SK Jr, et al: Distribution and correlates of sonographically detected carotid artery disease in the Cardiovascular Health Study. **Stroke** 23:1752–1760, 1992
 26. Pessin MS, Hinton RC, Davis KR, Duncan GW, Roberson GH, Ackerman RH, et al: Mechanisms of acute carotid stroke. **Ann Neurol** 6:245–252, 1979
 27. Redgrave JN, Lovett JK, Gallagher PJ, Rothwell PM: Histological assessment of 526 symptomatic carotid plaques in relation to the nature and timing of ischemic symptoms: the Oxford plaque study. **Circulation** 113:2320–2328, 2006
 28. Rothwell PM, Gibson R, Warlow CP: Interrelation between plaque surface morphology and degree of stenosis on carotid angiograms and the risk of ischemic stroke in patients with symptomatic carotid stenosis. On behalf of the European Carotid Surgery Trialists' Collaborative Group. **Stroke** 31:615–621, 2000
 29. Rothwell PM, Villagra R, Gibson R, Donders RC, Warlow CP: Evidence of a chronic systemic cause of instability of atherosclerotic plaques. **Lancet** 355:19–24, 2000
 30. Sundt TM, Sandok BA, Whisnant JP: Carotid endarterectomy. Complications and preoperative assessment of risk. **Mayo Clin Proc** 50:301–306, 1975
 31. Sundt TM Jr, Houser OW, Fode NC, Whisnant JP: Correlation of postoperative and two-year follow-up angiography with neurological function in 99 carotid endarterectomies in 86 consecutive patients. **Ann Surg** 203:90–100, 1986
 32. Tanimoto S, Ikari Y, Tanabe K, Yachi S, Nakajima H, Nakayama T, et al: Prevalence of carotid artery stenosis in patients with coronary artery disease in Japanese population. **Stroke** 36:2094–2098, 2005
 33. Virmani R, Ladich ER, Burke AP, Kolodgie FD: Histopathology of carotid atherosclerotic disease. **Neurosurgery** 59 (5 Suppl 3):S3-219–227, S3-3–13, 2006
 34. Wang X, Reape TJ, Li X, Rayner K, Webb CL, Burnand KG, et al: Induced expression of adipophilin mRNA in human macrophages stimulated with oxidized low-density lipoprotein and in atherosclerotic lesions. **FEBS Lett** 462:145–150, 1999
 35. Wasserman BA, Wityk RJ, Trout HH III, Virmani R: Low-grade carotid stenosis: looking beyond the lumen with MRI. **Stroke** 36:2504–2513, 2005
 36. Yuan C, Mitsumori LM, Ferguson MS, Polissar NL, Echelard D, Ortiz G, et al: In vivo accuracy of multispectral magnetic resonance imaging for identifying lipid-rich necrotic cores and intraplaque hemorrhage in advanced human carotid plaques. **Circulation** 104:2051–2056, 2001

Manuscript submitted March 17, 2010.

Accepted August 31, 2010.

Please include this information when citing this paper: published online October 1, 2010; DOI: 10.3171/2010.8.JNS10423.

Address correspondence to: Hiroyuki Hao, M.D., Ph.D., Department of Surgical Pathology, Hyogo College of Medicine, 1-1 Mukogawa-cho, Nishinomiya, Hyogo 663-8501, Japan. email: haohiro@hyo-med.ac.jp.

頸部放射線照射後の頸動脈狭窄症に対するステント留置術

江頭 裕介¹⁾, 佐藤 徹¹⁾, 梶田 宏輔¹⁾, 大川 将和¹⁾, 大西 宏之¹⁾, 岡崎 貴仁¹⁾,
高橋 淳¹⁾, 村尾 健一²⁾, 飯原 弘二¹⁾, 宮本 享³⁾

Carotid Artery Stenting for Radiation-induced Carotid Stenosis

Yusuke EGASHIRA¹⁾, Tetsu SATOW¹⁾, Kosuke MASUDA¹⁾, Masakazu OKAWA¹⁾, Hiroyuki OHNISHI¹⁾, Takahito OKAZAKI¹⁾,
Jun C TAKAHASHI¹⁾, Ken-ichi MURAO²⁾, Koji IIHARA¹⁾, and Susumu MIYAMOTO³⁾

Key words :

carotid artery stenosis,
radiation induced,
stenting,
unstable plaque,
complication

Purpose and Methods: To evaluate the outcome and lesion characteristics in patients with radiation induced carotid stenoses (RI-CS) treated by carotid artery stenting (CAS), a total of five patients with RI-CS (six lesions) were retrospectively analyzed.

Results: Four lesions had their most stenotic site at the common carotid artery (CCA). All cases had contralateral carotid or vertebral artery stenosis (>50%). All patients had risk factors of atherosclerosis and all lesions contained unstable plaques at the stenotic site. A total of seven procedures were carried out and procedural success was obtained in all cases. Asymptomatic embolic infarctions associated with procedure were observed in four cases by diffusion-weighted MR imaging. In-stent thrombi were observed in two cases, one of which developed a neurological symptom three days after the procedure.

Conclusion: CAS is a technically successful intervention for RI-CS. Care should be taken according to the characteristics of the plaque, which usually is vulnerable and long. Appropriate choice of a protection method could help in the reduction of unfavorable embolic complications and close postoperative follow up is mandatory.

(Received : March 10, 2010, Accepted : May 21, 2010)

No Shinkei Geka 38(10): 913 - 920, 2010

I. はじめに

頸部放射線照射後の頸動脈狭窄症 (radiation induced carotid stenosis : RI-CS) は、よく知られた合併症であり、現在ではステント留置術 (carotid artery stenting : CAS) が治療の第一選択とされている。しかしながら、その治療成績については報

告によってやや差異があり、いまだ統一された見解は得られていない。今回われわれは、自験例より RI-CS における病変の特徴、治療成績について検討を行い、治療に際しての留意点について考察を加えた。

*(2010. 3. 10 受稿, 2010. 5. 21 受理)

1) 国立循環器病研究センター脳神経外科, Department of Neurosurgery, National Cerebral and Cardiovascular Center

2) 城山病院脳血管内治療科, Department of Interventional Neuroradiology, Shiroyama Hospital

3) 京都大学脳神経外科, Department of Neurosurgery, Kyoto University

[連絡先] 江頭裕介 = 岐阜大学脳神経外科 (〒501-1194 岐阜市柳戸 1-1)

Corresponding author : Yusuke EGASHIRA, M.D., Department of Neurosurgery, Gifu University, 1-1 Yanagido, Gifu-city, Gifu 501-1194, JAPAN

Table 1 Characteristics of patients (n=5)

Case No.	Age, y/ Sex	Interval*/ Malignancy	Co-morbidities
1	79/M	6y/pharyngeal ca	HT, Sm
2	62/M	10y/laryngeal ca	HT, DM, HLP
3	74/M	15y/lymphoma	HT, HLP
4	79/M	22y/lymphoma	HLP
5	69/M	26y/lymphoma	HT, HLP

[Abbreviations] M: male, Ca: carcinoma, HT: hypertension, Sm: smoker, DM: diabetes mellitus, HLP: hyperlipidemia

*interval from irradiation to treatment

II. 対象と方法

2004年1月より2008年5月の間に当科にてCASを施行した連続55例のうち、過去に頸部に対する放射線照射の既往のあった5症例6血管に対する7手技を対象とした。全例男性で平均年齢72.6歳(62~79歳)、最狭窄部の平均狭窄率は70.8%(50~90%)であった。頸部放射線照射の実施後、CASまでの期間は平均16年(6~26年)であった。放射線照射が行われた原疾患は頸部悪性リンパ腫が3例、中咽頭癌が1例、喉頭癌が1例であった。いずれの症例も放射線照射後かなりの時間が経過しており、放射線照射範囲および照射線量についての詳細は調査不可能であった。全例で術前に脳血管撮影および頸部血管エコー(US)、MRIによる病変部のプラーク性状評価を行っており、術前評価項目として最狭窄部の局在、狭窄率、プラーク性状について検討した。MRIによるプラーク性状評価については、Siemens社製MAGNETOM Sonata 1.5 Tを使用し、magnetization-prepared rapid acquisition with gradient echo(MPRAGE)法⁹⁾にて狭窄部位のintensityを評価した。プラークのMPRAGE法によるhyperintensityとは胸鎖乳突筋の2倍以上のintensityを呈するcomponentをもつものと定義した。また治療後には神経症候の評価、MRI、脳血管撮影もしくは三次元CT血管造影、頸部血管エコーを行い、再狭窄ならびに経過観察中の脳虚血症候の発生の有無について検討した。

III. 結 果

対象症例群のprofileについてはTable 1に、病変のprofileについてはTable 2に示す。最狭窄部は総頸動脈(common carotid artery: CCA)のものが4例、内頸動脈(internal carotid artery: ICA)のものが2例であった。全例で対象としたRI-CS以外にも頸部主幹動脈の狭窄性病変を有していた。また、全例が動脈硬化の危険因子を有しており、4例では複数の危険因子を有していた。過去に同側の脳虚血発作もしくは一過性黒内障の既往のある症候性病変は4病変、無症候性病変は2病変であった。術前の評価においてはエコー上mobile plaqueを3病変で認め、MPRAGE法にてhyperintensityを呈するプラークは6病変すべてで認められ、いずれも不安定プラークを示唆する所見と考えられた。以上の病変に対し、計7回のCASを施行した。術前より2剤の抗血小板剤の内服および術中の抗凝固療法を行い、全例embolic protection device (EPD)使用下に手技を施行した(distal protection 6回、proximal protection 1回)。使用したEPDはPercuSurge Guardwire Plus[®] (GWP) (Medtronic Inc., Santa Rosa, CA, USA) 5回、ANGIOGUARD[®] XP (Cordis, Miami, FL, USA) 1回、Patlive[®] (クリニカルサプライ、岐阜) 1回(proximal protection)であり、全身麻酔下に2回、局所麻酔下に5回の手技が行われた。使用したステントの内訳はSMARTeR[®] (Cordis, Miami, FL, USA) 1、PRECISE[®] (Cordis, Miami, FL, USA) 2、Wallstent[®] RP (Boston Scientific, Natick, MA, USA) 2、Xpert[®] (Abbott vascular devices, Santa Clara, CA, USA) 1、Luminexx[®] (C. R. Bard, Convington, GA, USA) 1であった。7回すべての手技でステント留置に成功し、全例でほぼ完全な拡張を得た。7回の手技において術翌日のMRI (DWI) では、4回(57%)で新たな虚血性病変の出現がみられたが、いずれも無症状であった(Table 3)。術後30日以内の症候性脳梗塞は1例(14%)に認められ、術後3日目に遅発性の脳梗塞を来し、エコー上ステント内にmobile plaqueの出現が確認された症例であった。その他、いずれも無症候ではあるものの、術後6日目にステン

Table 2 Characteristics of lesions (n=6)

Case No.	Lesion No.	Most stenotic site/ % stenosis	presentation	MPRAGE high*	Mobile plaque**	Contralateral or vertebral lesion
1	1	L-CCA/65	asymptomatic	+	-	yes
2	2	L-ICA/90	asymptomatic	+	+	yes
	3	R-CCA/60	minor stroke	+	+	yes
3	4	L-CCA/50	minor stroke	+	+	yes
4	5	L-ICA/85	BRAO	+	-	yes
5	6	R-CCA/75	amaurosis fugax	+	-	yes

[Abbreviations] L: left, R: right, BRAO: branch retinal artery occlusion

*plaque hyperintensity on MPRAGE-sequence

**mobile plaque on carotid ultrasonography

Table 3 Procedural results (n=7)

technical success	7 (100%)
anesthesia	
local	5 (71%)
general	2 (29%)
embolic protection	
distal protection	6 (86%)
proximal protection	1 (14%)
materials	
SMARTeR®	1
PRECISE®	2
Wallstent® RP	2
Xpert®	1
Luminexx®	1

Table 4 Clinical outcomes (mean f/u 14mos)

embolic complication	4/7 (57%)
asymptomatic	4/4
≤30 days stroke after CAS	1/7 (14%)
in-stent thrombus	2/7 (29%)
reintervention	1/7 (14%)
restenosis (≥50%)	0/7 (0%)
patency rate	7/7 (100%)

ト内血栓を認め、経皮的血管拡張術 (percutaneous transluminal angioplasty : PTA) を要した1例、および術後6カ月後に同側大脳半球の新たな脳梗塞が確認された1例があった。平均14カ月のfollow upにて50%以上の再狭窄を呈した例はなく、全例で良好なステントの開存が確認された (Table 4)。

IV. 代表的症例

〈症例1〉 69歳 男性

既往歴 42歳時に頸部悪性リンパ腫に対し放射線照射を施行された。また、2006年4月に右頭頂葉の皮質梗塞のため他院で入院加療を受けている。

現病歴 2007年3月頃より特に起立時などに両側の眼前暗黒感を頻回に自覚するようになった。同年7月に当院にて精査を行ったところ、右

CCAの75%狭窄および左CCA閉塞、両側椎骨動脈閉塞、右鎖骨下動脈狭窄(75%)が判明した。MPRAGE法によるプラーク評価では狭窄部は著明なhyperintensityを呈しており (Fig. 1A)、不安定プラークの存在が疑われた。血管撮影上両側大脳半球は右ICAのみから灌流されている状態であった (Fig. 1B)。

治療方針 同部からのembolic strokeの予防、ならびに脳灌流圧の上昇を図るため、同部に対しCASを施行する方針とした。GWPによるdistal protection下に行うこととし、血流一時遮断に備え全身麻酔にて手技を行った。右大腿部に8Fr、右上腕に5Frのシースを留置し、CCAへのステント留置後にはアクセスが困難となる右鎖骨下動脈へのステント留置 (PALMAZ® φ8mm×25.1mm; Cordis, Miami, FL, USA) をCASに先立って施行した。CASの際の8Frガイディングカテーテル (Brite Tip®; Cordis, Miami, FL, USA) は誘導の際にCCAの狭窄部を通過せぬよう右上腕へとpull throughさせたガイドワイヤーを通し

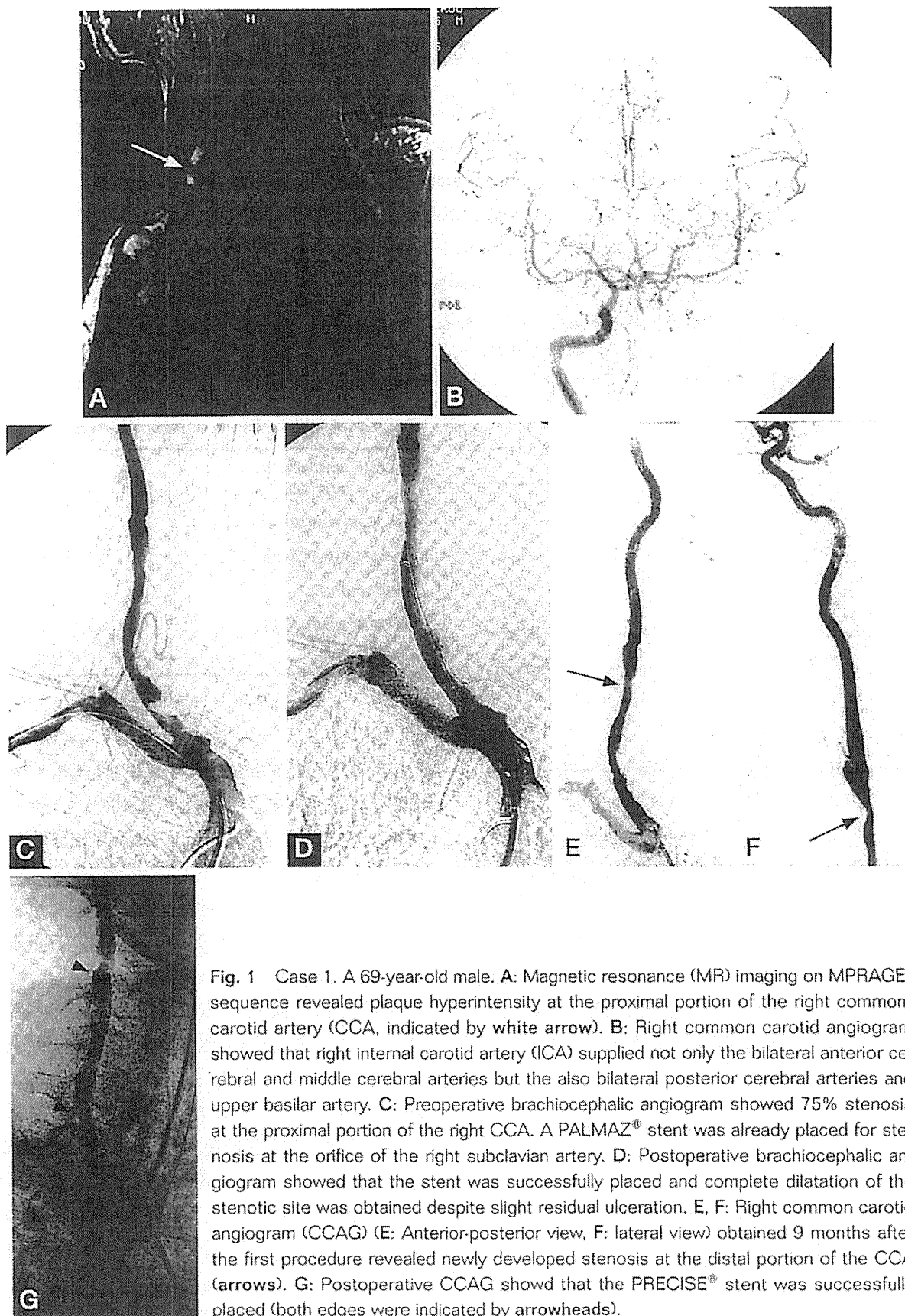


Fig. 1 Case 1. A 69-year-old male. **A:** Magnetic resonance (MR) imaging on MPRAGE-sequence revealed plaque hyperintensity at the proximal portion of the right common carotid artery (CCA, indicated by white arrow). **B:** Right common carotid angiogram showed that right internal carotid artery (ICA) supplied not only the bilateral anterior cerebral and middle cerebral arteries but the also bilateral posterior cerebral arteries and upper basilar artery. **C:** Preoperative brachiocephalic angiogram showed 75% stenosis at the proximal portion of the right CCA. A PALMAZ[®] stent was already placed for stenosis at the orifice of the right subclavian artery. **D:** Postoperative brachiocephalic angiogram showed that the stent was successfully placed and complete dilatation of the stenotic site was obtained despite slight residual ulceration. **E, F:** Right common carotid angiogram (CCAG) (**E:** Anterior-posterior view, **F:** lateral view) obtained 9 months after the first procedure revealed newly developed stenosis at the distal portion of the CCA (arrows). **G:** Postoperative CCAG showed that the PRECISE[®] stent was successfully placed (both edges were indicated by arrowheads).

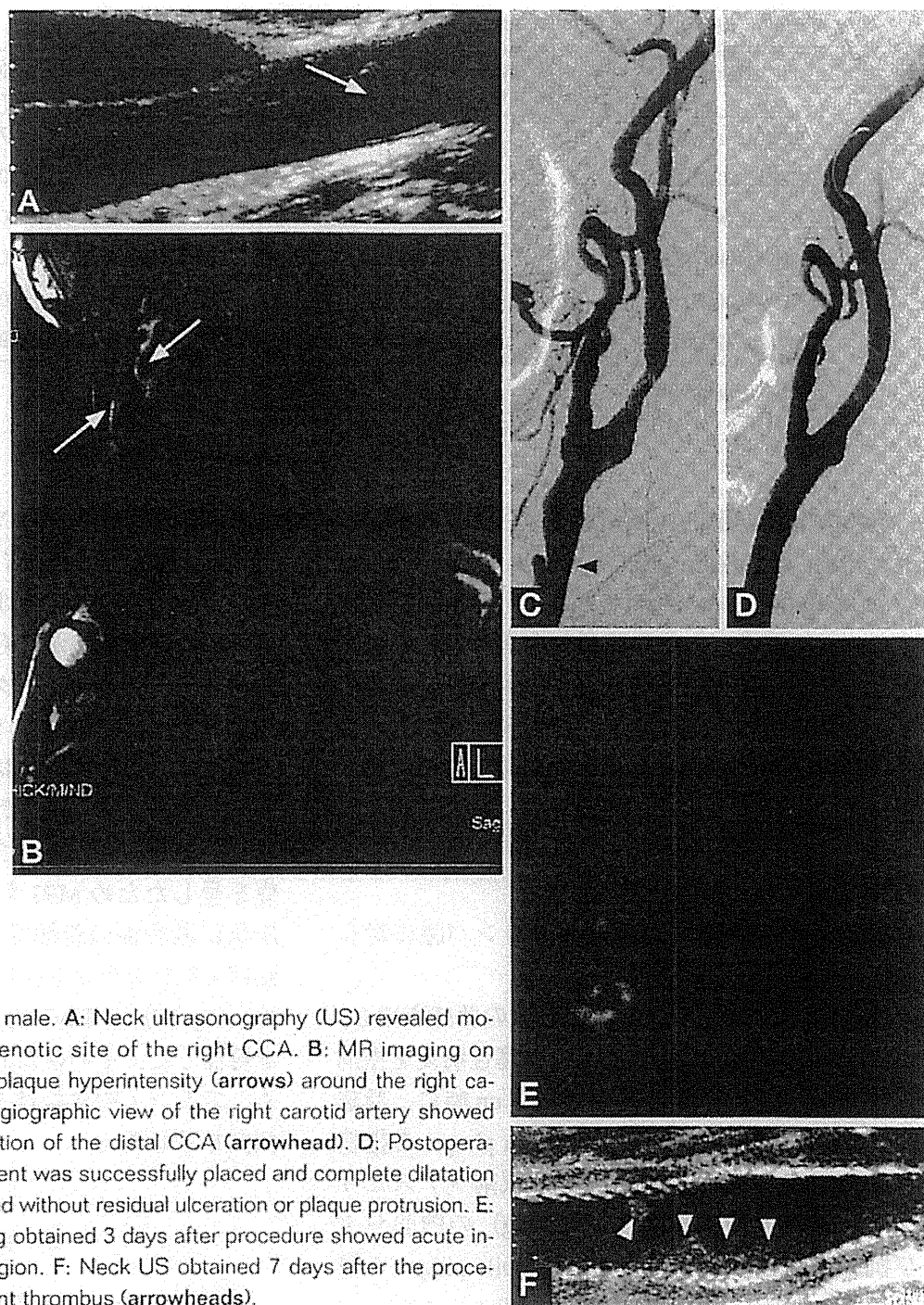


Fig. 2 Case 2. A 74-year-old male. A: Neck ultrasonography (US) revealed mobile plaque (arrow) at the stenotic site of the right CCA. B: MR imaging on MPRAGE-sequence revealed plaque hyperintensity (arrows) around the right carotid bifurcation. C: Lateral angiographic view of the right carotid artery showed moderate stenosis with ulceration of the distal CCA (arrowhead). D: Postoperative CCAG showed that the stent was successfully placed and complete dilatation of the stenotic site was obtained without residual ulceration or plaque protrusion. E: Diffusion-weighted MR imaging obtained 3 days after procedure showed acute infarction at the right parietal region. F: Neck US obtained 7 days after the procedure revealed a massive in-stent thrombus (arrowheads).

て誘導，腕頭動脈で安定させ，GWPによるdistal protectionを行った。狭窄部のproximalについては腕頭動脈までステントを留置することとし，12 mm径のLuminexx® (φ12 mm×60 mm)を選択した。これにより良好な拡張が得られた (Fig. 1C, D)。

術後経過 術翌日のMRIでは明らかな塞栓性合併症の所見は認めず，術前にみられた眼前暗黒

感などの症状は消失した。術後3カ月目のfollow upではステントの開存は良好であったが，ステントの遠位端よりさらに15 mmほど遠位に新たなmobile plaqueの出現を認めた。抗血小板療法を継続していたが，経時的に同部の狭窄の進行(70%)を認めたため (Fig. 1E, F)，無症状であったが初回術後9カ月目に再度全身麻酔下に同部に対しCASを行った。

Table 5 CAS for RI-CS: literature review

Series	No. of patients	Mean f/u*	Technical success	Perioperative mortality	Perioperative morbidity	<30 days stroke	Restenosis
Al-Mubarak (2000)	14	18	100%	0%	7%	7%	0%
Houdart (2001)	7	8	100%	0%	0%	0%	0%
Ting (2004)	16	30	94%	6%	12%	6%	17%
Harrod-Kim (2005)	16	28	100%	0%	4%	0%	21%
Cohen (2005)	8	16	100%	0%	0%	0%	0%
Protack (2007)	23	14	92%	0%	4%	9%	39%

*f/u=follow up months

治療方針 (2回目)・術後経過 2回目の手技については、全身麻酔、ANGIOGUARD® XP ϕ 6 mm による distal protection 下に行い、PERCISE® ϕ 10 mm \times 40 mm を前回留置したステントの遠位端と一部重なる形で留置した (Fig. 1G)。術後明らかな塞栓性合併症はなく、その後は6カ月の経過観察期間中に脳虚血発作および再狭窄の所見は認めていない。

〈症例2〉 74歳 男性

既往歴 59歳時に右頸部悪性リンパ腫に対し他院にて放射線照射を受けた。

現病歴 2006年8月に右前頭葉の梗塞を来し、この際に右ICAおよびCCAに潰瘍性病変を指摘されていた。2007年2月のfollow up時に、頸部USにて右CCAの狭窄部に mobile plaque を指摘された (Fig. 2A)。2剤の抗血小板剤 (アスピリン 100 mg+クロピドグレル 75 mg) の内服および抗凝固療法を施行されたが mobile plaque の消退が得られず、無症候性ながらMRIにて散在性の新鮮梗塞巣が確認されたため、加療目的で当科に紹介となった。脳血管撮影上は右CCAに50%狭窄、ICA起始部に50%狭窄および左CCAに40%狭窄、左椎骨動脈起始部に60%狭窄を認めた。MPRAGE上プラークはやはり著明な hyperintensity を呈していた (Fig. 2B)。

治療方針 CAS手技は右大腿動脈より8Fr Brite Tip® をCCAに留置し、GWPによるdistal protection下にて施行した。ICA病変に対しPTA (Amiia® ϕ 5.0 mm \times 20 mm; Cordis, Miami, FL,

USA) を施行後2本のWallstent® RP (ϕ 10 mm \times 39 mm および ϕ 9 mm \times 35 mm) を一部重ねる形でCCAからICAにかけて留置した。これにより病変部の完全拡張が得られ、潰瘍性病変の残存、ステント内へのプラークの突出などの異常所見は認めなかった (Fig. 2C, D)。

術後経過 術直後には新たな神経症状の出現はなく、術翌日のMRIでも明らかな塞栓性合併症は認めなかった。術後3日目に軽度の左不全片麻痺を呈したためMRIを再検したところ、頭頂葉皮質に散在性の新鮮梗塞像を認めた (Fig. 2E)。頸部USでステント内血栓の所見が認められたため (Fig. 2F)、2剤の抗血小板剤に加え抗凝固療法を再開した。その後新たな脳虚血症候の出現はなく、ステント内血栓は7カ月の経過で徐々に退縮傾向を示した。

V. 考 察

1. RI-CS に対する外科的治療

頸部への放射線照射は頸動脈狭窄の重要な危険因子としてよく知られており、その出現頻度は、Brownら²⁾によれば照射後7.5年で18%、Steeleら¹⁰⁾によれば10年で40%とされている。外科的治療については血栓内膜剝離術 (carotid endarterectomy: CEA) においては周囲組織との癒着などから剝離操作が困難であり、脳神経麻痺や創部感染の頻度が高いとされている⁶⁾。近年では通常CASが治療の第一選択となりつつあり、治療成績について論じた報告も散見される^{1,4,5,7,9,11)}。週

去の報告例における治療成績を Table 5 に示した。手技の成功率や周術期の虚血性合併症についてはほぼ共通して良好な成績が得られている。ただし Protack らの報告⁹⁾においては、通常の動脈硬化性病変に対する CAS の成績と比較し有意に再狭窄の頻度が高く、通常の CAS においては 9% であったのに対し RI-CS における頻度は 39% にのほり、また再狭窄までの期間も平均 0.92 年と通常の CAS と比較して短い傾向にあった。再治療例も通常の CAS における 1% に対し、RI-CS 例では 13% と有意差をもって多かったとしている。本症例群においては平均 14 カ月の経過観察期間において有意な再狭窄を呈した症例はなかったが、2 例 (29%) で遅発性にステント内血栓を認め、1 例 (14%) では同一血管の他部位に新たな狭窄の進行を認めた。これらの結果から、RI-CS に対する CAS では、術後短期間でのステント内血栓やステント内のみならずその近傍での再狭窄に十分に注意すべきであろうと考えられた。

2. RI-CS における病変の特徴

本研究においては、MRI および頸部 US での狭窄部のプラーク性状評価の検討からは全例で不安定プラークが疑われる所見を認めた (MPRAGE での hyperintensity 6 例、頸部 US 上の mobile plaque 3 例)。RI-CS における病理学的、US 上の所見は動脈硬化性病変と同様であると報告されており³⁾、放射線照射が動脈硬化性変化を促進する因子であろうと考えられている⁹⁾。本症例群では全例が動脈硬化の危険因子を有しており、この結果は過去の報告⁹⁾と同様の傾向であった。これらの結果からも、頸部放射線照射後長期間が経過してから顕在化する (つまり患者の年齢も高齢化している) RI-CS においては、動脈硬化が病変の進展に強く関与している可能性、あるいは放射線照射が動脈硬化を促進している可能性が考えられる。本研究でわれわれが病変評価に用いた MRI (MPRAGE 法) において、プラーク内の高信号は不安定プラークと考えられる所見であり¹³⁾、MPRAGE 法は RI-CS の病変の性状評価の方法として通常の動脈硬化性病変の場合と同様に protection method およびステント選択の上で、非常

に有用であろうと考えている。

病変の局在については当然放射線照射野との関連が大きいと考えられるが、今回の検討と同様に CCA もしくは CCA から ICA にかけての長い segment で狭窄性変化を起こす症例が多いようである^{4,5,9)}。前述の症例 1 のように、通常の CAS と比較してより近位の CCA に病変を有する場合にはガイディングカテーテルの誘導の際のプラークの損傷や留置に際しての安定性が問題となり得るため、より慎重なデバイスの操作が要求される。また、対側もしくは椎骨動脈病変も今回の検討では全例に合併しており、文献上も 31 ~ 48% と高頻度に併存する^{4,5,9)}。近年 CAS においては routine に EPD が使用されるようになり、RI-CS に対する CAS においても EPD は必須のデバイスと考えられているが⁴⁾、その使用に際しては一時的な血流遮断または血流減少が生じ得るため、特に複数の併存病変を有する例では、全身麻酔での手技や血流遮断をできるだけ短くするような治療手技が要求される。

VI. 結 語

RI-CS に対する CAS においては、術前に詳細な検討を行えば手技そのものに難渋することは少なく、全例でステント留置が可能であり、良好な拡張が得られた。ただしプラーク性状や併存病変の存在からは CAS に際してはより慎重な手技、周術期の経過観察が要求される。中長期成績についてはいまだ明らかではなく、RI-CS に対する CAS の真の有効性を明らかにするためには、より多くの症例研究および長期の経過観察が必要と思われた。

文 献

- 1) Al-Mubarak N, Roubin GS, Iyer SS, Gomez CR, Liu MW, Vitek JJ : Carotid stenting for severe radiation-induced extracranial carotid artery occlusive disease. *J Endovasc Ther* 7 : 36-40, 2000
- 2) Brown PD, Foote RL, McLaulhin MP, Halyard MY, Ballman KV, Collie AC, Miller RC, Flemming KD, Hallett JW : A historical prospective cohort study of carotid artery stenosis after

- radiotherapy for head and neck malignancies. *Int J Radiat Oncol Biol Phys* 63 : 1361-1367, 2005
- 3) Cheng SW, Ting AC, Wu LL : Ultrasonic analysis of plaque characteristics and intimal-medial thickness in radiation induced atherosclerotic carotid arteries. *Eur J Endovasc Surg* 24 : 499-455, 2002
 - 4) Cohen JE, Rajz G, Lylyk P, Ben-Hur T, Comori JM, Umansky F : Protected stent-assisted angioplasty in radiation-induced carotid artery stenosis. *Neurol Res* 27 (Supple 1) : S69-S72, 2005
 - 5) Harrod-Kim P, Kadkhodayan Y, Derdeyn CP, Cross DT 3rd, Moran CJ : Outcomes of carotid angioplasty and stenting for radiation-associated stenosis. *AJNR Am J Neuroradiol* 26 : 1781-1788, 2005
 - 6) Hassen-Khodja R, Sala F, Declémy S, Lagrange JL, Bouillane PJ, Batt M : Surgical management of atherosclerotic carotid artery stenosis after cervical radiation therapy. *Ann Vasc Surg* 14 : 608-611, 2000
 - 7) Houdart E, Mounayer C, Chapot R, Saint-Maurice JP, Merland JJ : Carotid stenting for radiation-induced carotid stenoses : a report of 7 cases. *Stroke* 32 : 118-121, 2001
 - 8) Mugler JP 3rd, Brookeman JR : Three-dimensional magnetization-prepared rapid gradient-echo imaging (3D MP RAGE). *Magn Reson Med* 15 : 152-157, 1990
 - 9) Protack CD, Bakken AM, Saad WA, Illig KA, Waldman DL, Davies MG : Radiation arteritis : A contraindication to carotid stenting? *J Vasc Surg* 45 : 110-117, 2007
 - 10) Steele SR, Martin MJ, Mullenix PS, Crawford JV, Cuadrado DS, Andersen CA : Focused high-risk population screening for carotid arterial stenosis after radiation therapy for head and neck cancer. *Am J Surg* 187 : 594-598, 2004
 - 11) Ting AC, Cheng SW, Yeung KM, Cheng PW, Lui WM, Ho P, Tso WK : Carotid stenting for radiation-induced extracranial carotid artery occlusive disease : efficacy and midterm outcomes. *J Endovasc Ther* 11 : 53-59, 2004
 - 12) Yamada N, Higashi M, Otsubo R, Sakuma T, Oyama N, Tanaka R, Iihara K, Naritomi H, Minematsu K, Naito H : Association between signal hyperintensity on T1-weighted MR imaging of carotid plaques and ipsilateral ischemic events. *AJNR Am J Neuroradiol* 28 : 287-292, 2007

好評書発売中

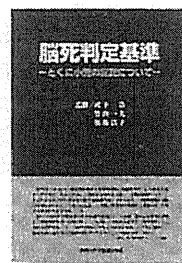
脳死判定基準 —とくに小児の脳死について—

監修=武下 浩 山口大学名誉教授
竹内一夫 杏林大学名誉教授
加藤浩子 有馬温泉病院(副院長)

今日、脳死は医学的、臨床的に確立された概念であり、脳死判定基準によって脳死と判定されれば、それをもって人の死とするのが多くの先進諸国に共通した考えである。

- | | |
|--------------------|---------------------------------|
| 第1章 脳死概念の発達 | 第6章 小児脳死判定基準 |
| 第2章 意識の発達と意識障害 | 第7章 小児脳死判定の補助検査 |
| 第3章 脳死の病態生理 | 第8章 長期脳死と脊髄活動 |
| 第4章 脳死による全身の病態生理反応 | 第9章 小児脳死判定基準の周辺課題 |
| 第5章 小児脳死の原因疾患 | 第10章 アジア諸国とドイツ、カナダ、スイスの小児脳死判定基準 |

● B5判 112頁 定価 3,675円(本体 3,500円 + 5% 税) ISBN 978-4-88003-835-3



手術・麻酔後の高次脳機能障害

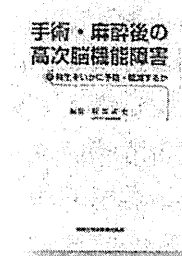
—発生をいかに予防・軽減するか—

編集=坂部武史 山口労災病院院長

術後の高次脳機能障害の発生を予防・軽減し、患者のQOLを高めるための周術期管理の向上に役立て、今後の課題・方向性を示した。

総論 手術後の高次脳機能障害 —何が問題か?なぜ問題か?—/高次脳機能障害 —神経内科の立場から—/高次脳機能障害の検査法/麻酔薬の中樞神経毒性/麻酔薬以外の薬剤による精神・行動障害
各論 心臓手術と高次脳機能障害/大血管手術と高次脳機能障害/非心臓手術における麻酔後の高次脳機能障害 —心臓手術との比較—/非心臓手術後の精神機能および認知機能障害 —高齢者、うつ病患者を中心に—/術後高次脳機能障害 —麻酔法の違いによる影響—/高次脳機能障害と術中モニター/術後高次脳機能障害とバイオマーカー/術後せん妄/術後高次脳機能障害とインフォームド・コンセント

● A5判 232頁 定価 4,725円(本体 4,500円 + 5% 税) ISBN 978-4-88003-832-2



〒106-0047 東京都港区南麻布2丁目8番18号
電話(03)3798-3315 FAX(03)3798-3096

真興交易(株)医書出版部

URL: <http://www.sshinko.com>
E-mail: info@sshinko.com

Assessment of necrotic core with intraplaque hemorrhage in atherosclerotic carotid artery plaque by MR imaging with 3D gradient-echo sequence in patients with high-grade stenosis

Clinical article

TOMOHIITO HISHIKAWA, M.D.,¹ KOJI IIHARA, M.D.,¹ NAOAKI YAMADA, M.D.,²
HATSUE ISHIBASHI-UEDA, M.D.,³ AND SUSUMU MIYAMOTO, M.D.¹

Departments of ¹Neurosurgery, ²Radiology, and ³Pathology, National Cardiovascular Center, Osaka, Japan

Object. The aim of this study was to assess the histopathological differences between advanced atherosclerotic carotid artery (CA) plaques with signal hyperintensity on T1-weighted MR images and those without, focusing on necrotic core size and intraplaque hemorrhage (IPH).

Methods. Thirty-five patients scheduled for carotid endarterectomy underwent preoperative CA MR imaging using 3D inversion-recovery-based T1-weighted imaging (magnetization-prepared rapid acquisition gradient-echo [MPRAGE]). The signal intensity of the CA plaque on MPRAGE sequences was classified as “high” when the intensity was more than 200% that of adjacent muscle. A total of 96 axial MR images obtained in 35 patients were compared with corresponding histological sections from 36 excised specimens. The area of the necrotic core in histological sections was compared between specimens with and without high signal intensity on MPRAGE sequences. The IPH was histopathologically graded according to the size of the area positive for glycoporphin A as revealed by immunohistochemical staining. The difference between plaques with and without high signal intensity was investigated with respect to the degree of IPH. The relationship of the severity of IPH to size of the necrotic core was also evaluated.

Results. The area of the necrotic core in plaques with high signal intensity on MPRAGE sequences was significantly larger than that in plaques without high signal intensity (median 51.2% [interquartile range 43.3–66.8%] vs 49.0% [33.2–57.6%], $p = 0.029$). Carotid artery plaques with high signal intensity had significantly more severe IPH than plaques with lower signal intensity ($p < 0.0001$). The severity of IPH was significantly associated with the size of the necrotic core ($p < 0.0001$).

Conclusions. Atherosclerotic CA plaques with high signal intensity on MPRAGE sequences had large necrotic cores with IPH in patients with high-grade stenosis; MPRAGE is useful for the evaluation of CA plaque progression. (DOI: 10.3171/2010.3.JNS091057)

KEY WORDS • carotid artery stenosis • intraplaque hemorrhage •
MR imaging • necrotic core

THE prophylactic effectiveness of CEA in patients with more than a certain degree of arterial stenosis has been proven in several randomized multicenter trials.^{7,8,11,21} Although the degree of lumen narrowing is a significant risk factor in stroke, the role of vulnerable CA plaque has recently been emphasized,²⁰ and some reports have demonstrated that episodes of cerebral ischemia in patients with CA lesions are not restricted to cases with severe stenosis.^{3,10,24} The type of vulnerable plaque that is most prone to rupture is characterized by a large necrotic core, a thin fibrous cap (< 65 μm thick), and widespread macrophage infiltration within the fibrous cap.³¹ In addition, the role of IPH in the vulnerability of CA plaques has been emphasized by many investigators.^{6,17,26,28,29,34}

Magnetic resonance imaging is well suited for CA plaque evaluation in a clinical setting because it is noninvasive and widely available, provides excellent soft tissue contrast, and does not involve ionizing radiation. In response to reports demonstrating the close association of IPH with cerebral ischemic events,²⁶ many authors have recently emphasized the value of IPH detection by MR imaging and have demonstrated the clinical usefulness of this noninvasive modality.^{1,6,13,17,28,29,33}

Our institute has routinely performed CA plaque MR imaging using 3D inversion-recovery-based T1-weighted sequences (MPRAGE) before interventions for CA stenosis. Yamada et al.³³ demonstrated that CA plaque with high signal intensity on MPRAGE sequences was significantly associated with previous ipsilateral ischemic events in patients with moderate and severe stenosis. In that report,

This article contains some figures that are displayed in color online but in black and white in the print edition.

Abbreviations used in this paper: CA = carotid artery; CEA = carotid endarterectomy; ICA = internal carotid artery; IPH = intraplaque hemorrhage; IQR = interquartile range; MPRAGE = magnetization-prepared rapid acquisition gradient echo.

Assessment of carotid artery plaque by MPRAGE

CA plaque signal intensity on greater than 200% that of adjacent muscles was defined as high and the chi values for interobserver and intraobserver agreement were 0.729 and 0.792, respectively (good agreement).³³ Taking the close association of MPRAGE signal intensity (using a threshold of 200% of the intensity of adjacent muscles) with symptomatology into consideration, we sought to determine the histopathological differences between CA plaques with and without high signal intensity as the next stage of investigation. The aim of this study was to retrospectively assess the vulnerability of CA plaques, focusing on differences in necrotic core area and degree of IPH between plaques that are associated with high signal intensity on MPRAGE sequences and those that are associated with lower signal intensity (< 200% of the intensity of adjacent muscle tissue).

Methods

Study Population

Thirty-five patients (32 men, 3 women) with a mean (\pm SD) age of 69.0 ± 7.8 years who were scheduled for CEA at our institute between May 2006 and March 2007 were included in this study. Patient characteristics were examined retrospectively through a review of the relevant medical records. A total of 36 CEAs for CA stenosis (1 patient had bilateral CA stenosis) were performed, and 36 endarterectomy specimens were analyzed. Twenty patients (57.1%) had a history of ipsilateral ischemic events, including cerebral infarction, transient ischemic attack, and retinal ischemia, within the previous 6 months, and their lesions were defined as symptomatic. The degree of CA stenosis was measured using digital subtraction angiography (17 lesions), 3D CT angiography (17 lesions), or contrast-enhanced MR angiography (2 lesions) according to the method used in the North American Symptomatic Carotid Endarterectomy Trial (NASCET).⁹ The criteria for CEA were 70% stenosis or greater for symptomatic cases and 75% stenosis or greater for asymptomatic cases.¹² All 36 endarterectomy specimens were circumferentially removed with the plaque intact.

Magnetic Resonance Imaging Protocol

Imaging was performed using standard neck array and spine array coils in a Magnetom Sonata 1.5-T system (Siemens). Plaque imaging was performed using MPRAGE in the transaxial section with null blood condition (effective inversion time 660 msec; TR 1500 msec) and the water excitation technique to suppress fat signals.³³ Other scanning parameters were as follows: TE 5.0 msec; FOV 180×180 mm; matrix 256×204 ; section thickness 1.25 mm; 56 partitions, covering 70 mm around the CA bifurcation; and data acquisition time 5 minutes. The mean interval between MR imaging and CEA was 17.9 ± 20.4 days. In symptomatic patients, the mean duration of time from last symptoms to MR imaging was 16.2 ± 27.0 days.

Image Review and Criteria

The MR images were reviewed by an experienced radiologist (N.Y.) blinded to clinical and pathological data.

The signal intensity of plaques on MPRAGE relative to the signal intensity in adjacent muscle (typically the sternocleidomastoid muscle)—referred to in this paper as the relative MPRAGE signal intensity—was calculated in each image at 5-mm intervals extending rostrally along the ICA from the CA bifurcation. Any section of plaque that displayed a signal intensity that was more than 200% that of the adjacent muscle tissue was categorized as having high signal intensity.

Endarterectomy Specimen Processing and Criteria

In symptomatic cases, the mean value of the time from most recent symptoms to CEA was 20.3 ± 28.1 days. The endarterectomy specimens were immediately fixed in Histochoice fixative (Amresco, Inc.) for 48 hours and decalcified with EDTA. Subsequently, they were divided into 5-mm blocks (starting at the CA bifurcation and extending rostrally along the ICA) and embedded in paraffin. From each 5-mm block, a 3- μ m section was obtained and stained with H & E and Masson trichrome for histological evaluation. In addition, immunohistochemical testing for glycoporphin A was performed to identify IPH (1:200 dilution; Dako). Each section was histopathologically evaluated by an experienced histopathologist (H.I.U.) who was unaware of the MR imaging results. Atheromatous plaques were defined as areas of protrusion into the vascular lumen due to atherosclerosis that were bounded by an internal elastic layer and included fibrous caps. Necrotic core was defined as a core area of atheromatous plaques that consisted of necrotic macrophages, cholesterol crystals, and sometimes hemorrhage. The proportion of the necrotic core area to the total plaque area (NC proportion) was measured using a computer-based morphometric system (WinRoof, Mitani Co.). As an index of the degree of IPH (IPH score), the ratio of the glycoporphin A-positive area to the total plaque area was calculated and the sample was graded according to the following scale: a ratio ≥ 0.40 corresponded to a score of 3; a ratio ≥ 0.20 and < 0.40 , a score of 2; a ratio < 0.20 , a score of 1.

Correlation of MR Imaging and Histological Specimens

The MR images and histological sections were independently reviewed and evaluated. The relative distance from the CA bifurcation was used as a landmark to match the histological data with the MR images in the longitudinal direction of the artery. Morphological features such as lumen size and shape were also used as a reference landmark.

Statistical Analysis

Quantitative variables are presented as the medians and IQRs. The correlation between the relative MPRAGE signal intensity and the NC proportion or IPH score was assessed by nonparametric analysis of the Spearman rank correlation test. The Mann-Whitney U-test was used to compare the NC proportion in samples with high signal intensity on MPRAGE sequences to the proportion in samples with lower signal intensity. Contingency tables displaying IPH scores and MPRAGE signal intensity

(high vs not high) were generated and analyzed by means of the chi-square test to determine a trend. The relationship of IPH score to NC proportion was assessed through nonparametric analysis using the Kruskal-Wallis test. All statistical analyses were performed with StatView (SAS Institute). Differences were considered to be significant when p values were < 0.05 .

Results

A total of 96 histological sections corresponding to MR images from 36 endarterectomy specimens were evaluated in this study. Table 1 shows the baseline characteristics of patients, including demographic variables and risk factors.

Correlation Between Size of Necrotic Core and MPRAGE Signal Intensity

Figure 1 shows a scatterplot of the relative MPRAGE signal intensity and the NC proportion. A significant positive correlation was found between the relative MPRAGE signal intensity and the NC proportion ($p = 0.0032$). The NC proportions in plaques with high signal intensity were significantly larger than those in plaques without high signal intensity (median 51.2% [IQR 43.3–66.8%] vs 49.0% [IQR 33.2–57.6%], $p = 0.029$; Fig. 2).

Relationship Between IPH and MPRAGE Signal Intensity

Figure 3 shows a scatterplot of the relative MPRAGE signal intensity and the IPH score. There was a significant positive correlation between the relative MPRAGE signal intensity and the IPH score ($p < 0.0001$). High signal intensity was seen in images corresponding to 14.3, 25.0, and 64.3% of specimens with IPH scores of 1, 2, and 3, respectively. Higher IPH score was significantly associated with high signal intensity on MPRAGE sequences ($p < 0.0001$; Table 2).

Relationship Between IPH and Necrotic Core

The median values (IQRs) for NC proportion were 32.7% (25.3–47.8%), 45.4% (40.5–54.8%), and 53.1% (47.4–65.6%) for samples with IPH scores of 1, 2, and 3, respectively. Higher IPH scores were significantly associated with larger necrotic cores ($p < 0.0001$; Fig. 4).

Representative Examples

Figures 5 and 6 show the representative appearance of MPRAGE images and histological findings from corresponding specimens.

Discussion

Role of IPH in Plaque Progression

Naghavi et al.¹⁹ proposed the concept of vulnerable patients, along with criteria for defining vulnerable plaques, based on autopsy studies of coronary arteries. Among their criteria, IPH has recently been emphasized in pathological studies as an important factor in CA plaque progression.^{14,15,32} It has been reported that

TABLE 1: Summary of demographic and clinical characteristics in 35 patients*

Characteristic	Value
symptomatic lesions	20 (57)
mean degree of stenosis (%)	80 ± 10
mean age in yrs	69 ± 8
female sex	3 (9)
hypertension	24 (69)
diabetes mellitus	15 (43)
hyperlipidemia	19 (54)
cigarette smoking	20 (57)

* Values represent numbers of patients (%) unless otherwise indicated. Means are presented ± SDs.

necrotic core enlargement is crucial for plaque rupture and that increased free cholesterol within the necrotic core is closely associated with lesion instability.³² Concerning the derivation of free cholesterol, it is generally accepted that apoptotic macrophages are an efficient source of free cholesterol in plaques,²⁷ although Kolodgie and colleagues^{15,32} have demonstrated new lines of evidence suggesting that erythrocyte membranes contribute a significant amount of the free cholesterol in coronary plaques. Nuotio et al.²² also reported that IPH could play a role in the vulnerability of symptomatic CA plaques by contributing to lipid accumulation and inducing adipophilin (an adipose differentiation-related protein) and further increasing lipid accumulation by preventing lipid efflux. From a symptomatological point of view, Lusby et al.¹⁶ demonstrated that a history of multiple hemorrhage (hemorrhages at various ages) was seen in 81% of patients with symptoms of cerebral ischemia associated with atherosclerotic CA stenosis.

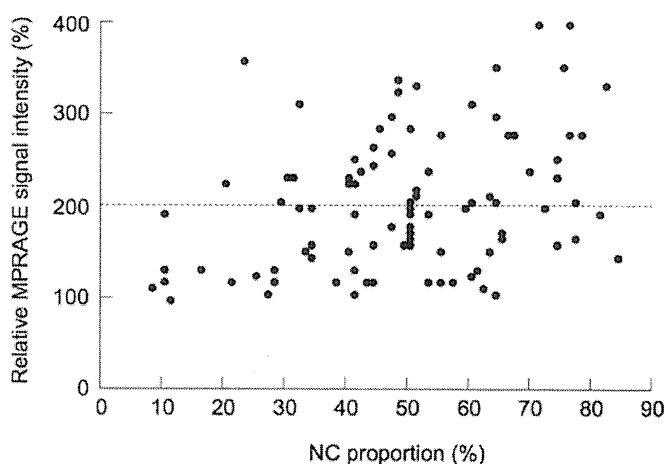


Fig. 1. Scatterplot showing the signal intensity of plaques on MPRAGE sequences relative to the signal intensity in adjacent muscle (relative MPRAGE signal intensity) and the proportion of the necrotic core (NC) area to the total plaque area (NC proportion) as established by pathological examination of specimens. The broken horizontal line indicates the level of 200% MPRAGE proportion, the threshold for "high" signal intensity in this study.

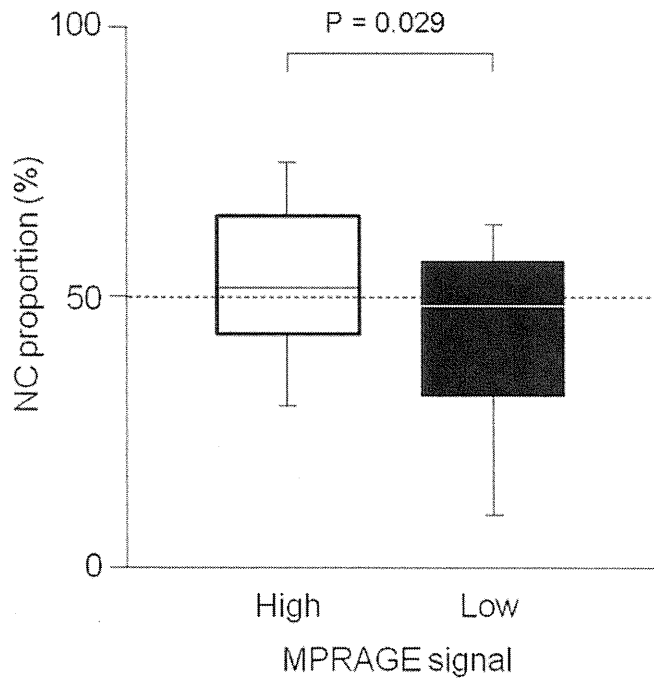


Fig. 2. Box and whisker plot showing the relationship of the NC proportion to MPRAGE signal intensity. The NC proportion in specimens corresponding to imaging studies that showed high signal intensity on MPRAGE sequences was significantly larger than that in specimens that showed lower signal intensity ($p = 0.029$, Mann-Whitney U-test). The broken horizontal line is at the level of 50% NC proportion.

The present study demonstrated a significant association of IPH with necrotic core in patients with high-grade CA stenosis. Therefore, the use of a noninvasive and objective modality to detect IPH and to predict subsequent

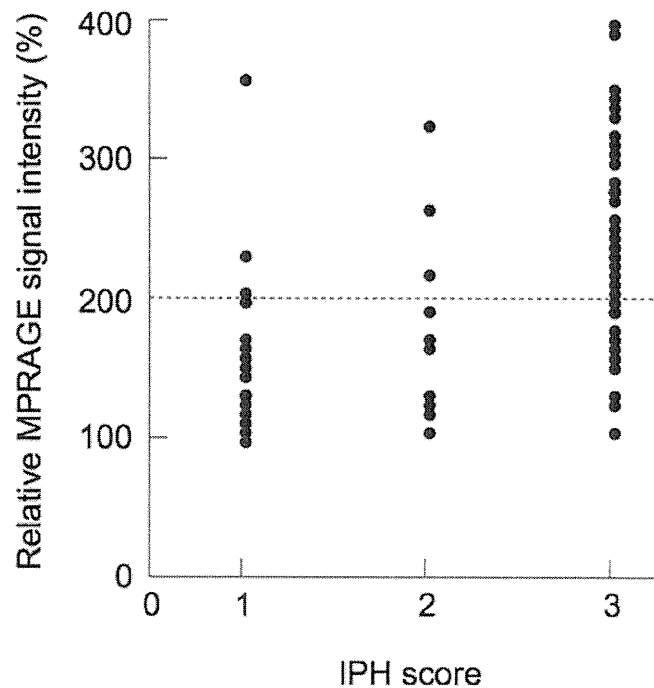


Fig. 3. Scatterplot showing the relative MPRAGE signal intensity and IPH score (1–3). The broken horizontal line is at the 200% threshold for high signal intensity.

TABLE 2: Correlation between high signal intensity on MPRAGE sequences in 96 axial MR images and IPH score in corresponding histological sections*

IPH Score	No. of MR Images	Relative Signal Intensity >200%		p Value
		Yes	No	
1	28	4 (14.3)	24 (85.7)	<0.0001
2	12	3 (25.0)	9 (75.0)	
3	56	36 (64.3)	20 (35.7)	

* Signal intensity in CA plaque was assessed relative to that of adjacent muscle tissue, using 200% as the threshold for "high" signal intensity on MPRAGE sequences. Values represent numbers of images, expressed as a percentage of the images in the given score category in parentheses.

necrotic core expansion in CA plaque could play an important role in assessing plaque vulnerability and in managing patients with CA stenosis in a clinical setting.

Assessment of Carotid Plaque by MPRAGE Sequence

Moody et al.¹⁷ used a T1-weighted magnetization-prepared 3D gradient echo sequence, a technique identical to that used in MPRAGE, to detect complicated plaque by detecting IPH in an in vivo study of CA plaques in symptomatic patients. Bitar et al.⁴ recently reported that MR imaging of IPH using a 3D spoiled gradient-echo sequence resulted in strong agreement between imaging and histologic findings. Yamada et al.³³ disclosed significant associations between cerebral ischemic events and MPRAGE hyperintensity according to stenosis severity using 200% of the signal intensity of adjacent muscle as the threshold for high signal intensity and reported the percentages of patients with high signal intensity were 21, 54, and 65% for mild (0–29%), moderate (30–69%), and severe (70–99%) stenosis, respectively. The present study demonstrated that the NC proportion in plaques with high signal intensity on MPRAGE sequences was significantly larger than that in plaques with lower signal intensity, and the severity of IPH was significantly correlated with signal intensity. The hemorrhage-rich larger necrotic core is a pathological basis for the high signal intensity on MPRAGE in these plaques, which has previously been shown to be significantly associated with symptomatology.³³ Also, in the present study, 58% of CAs examined (21 of 36) had high signal intensity on MPRAGE sequences and 58% of the endarterectomy sections (56 of 96) exhibited the highest degree of IPH (score of 3 in our pathological examination). Together with the data from Yamada et al.,³³ the data from this study shows, through the association between MPRAGE signal hyperintensity and high-grade CA stenosis, that IPH has a high prevalence in advanced CA atherosclerotic plaques; our data also raise the possibility that IPH is a major mechanism underlying the progression of stenosis through its stages of severity as well as the expansion of the necrotic core.

The majority of previous reports have used multiple contrast techniques (T1-weighted, T2-weighted, proton-density-weighted, and 3D time-of-flight MR imaging)

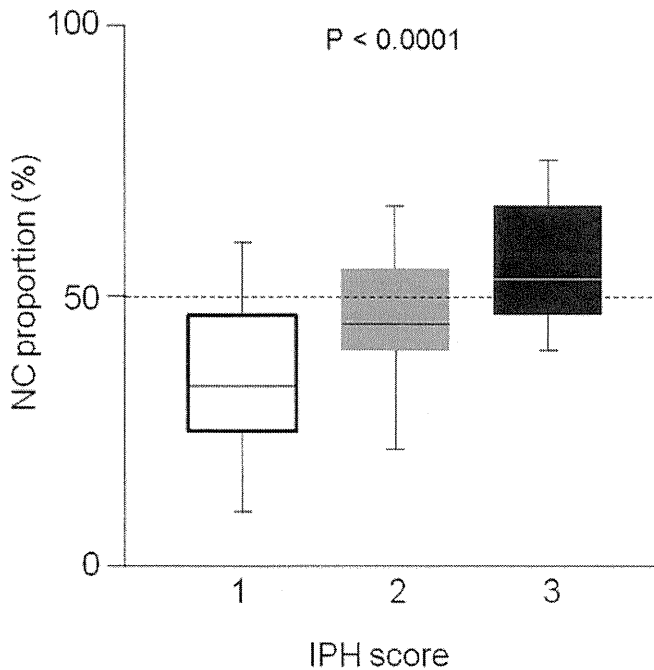


Fig. 4. Box and whisker plot showing the relation of IPH score to NC proportion. Higher IPH scores were significantly associated with higher NC proportion, according to the Kruskal-Wallis test ($p < 0.0001$). The broken horizontal line is at the level of 50% NC proportion.

to identify necrotic cores and IPH.^{6,13,28,29,34} Saam et al.²⁵ demonstrated the accuracy and reproducibility of using multicontrast imaging to quantify CA plaque components. On the other hand, the usefulness of single-contrast imaging using a 3D gradient-echo sequence has also been demonstrated.^{1,4,17,18,33} This sequence is often employed to identify IPH using a T1-weighted signal alone. In a study comparing the performance of a gradient-echo sequence with that of a spin-echo sequence, the gradient-echo sequence had a higher detection rate for IPH as well as much better interobserver agreement and better image quality.⁵ Likewise, Ota et al.²³ reported that the MPRAGE sequence at 3 T had the highest diagnostic capability for the detection and quantification of IPH, in a study comparing it with the fast spin echo and spoiled gradient echo sequences. In the present study, the area over which MPRAGE signal hyperintensity was present in CA plaque was not directly compared with the area of the necrotic core as measured through histopathological analysis. Nevertheless, our data reveal that the areas of high signal intensity on MPRAGE sequences coincide with the hemorrhage-rich large necrotic core. As the interpretation of MPRAGE signal intensity is simple and objective, requiring only a short image acquisition time (5 minutes), this 3D gradient-echo sequence technique is useful in a clinical setting.

As the practice of CA stent placement has rapidly become more prevalent, distal embolic complications during the procedure have become an important clinical issue. A report on the use of a filter protection device during CA stent placement in Japan revealed that disturbed blood flow presumably due to the blockage of the filter pores by plaque was observed in 40.0% of cases (slow flow in

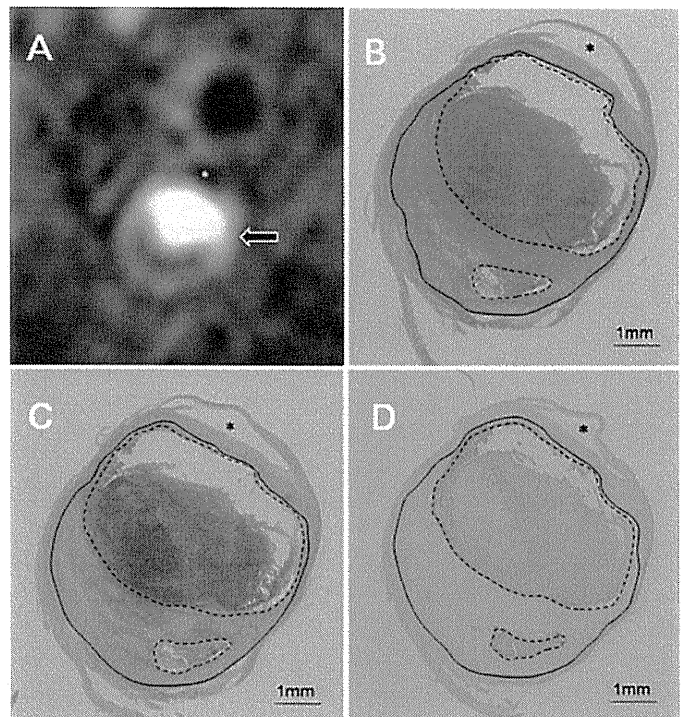


Fig. 5. An example of plaque with high signal intensity. **A:** An MPRAGE image showing the plaque (arrow). **B and C:** Photomicrographs of histological sections showing a large amount of necrotic core with IPH. H & E (**B**) and Masson trichrome (**C**). **D:** Photomicrograph showing that the necrotic core is strongly positive for glycoprotein A. Asterisks indicate the ICA lumen. The total plaque area is delineated by a solid line and the necrotic core area by a dotted line. Bar = 1 mm.

26.7%, no flow in 13.3%).³⁰ Angeneli et al.² collected the embolized debris caught in such a filter and performed histopathological analysis on it; they reported that the collected debris consisted predominantly of thrombotic material, foam cells, and cholesterol clefts. The use of MPRAGE for CA plaque analysis before CA stent placement could be useful in predicting the risk of embolic complication and blood flow disturbances and could aid in selecting suitable distal protection devices.

Study Limitations

First, we used immunohistochemical staining for glycoprotein A as a marker of IPH. Glycoprotein A is a protein specific to erythrocytes that facilitates anion exchange; it is also an indicator of previous hemorrhage.¹⁵ Although high signal intensity on MPRAGE sequences was associated with the detection of previous hemorrhages by glycoprotein A, the signal hyperintensity may not be related to fresh thrombi or hemorrhages. In fact, in this study, a few endarterectomy sections with fresh thrombi revealed only lower-intensity signals. Because fresh thrombi play a crucial role in the pathogenesis of stroke,²⁶ it is important to detect them and to accurately classify IPH; thus, if MPRAGE is to become a useful technique, we must develop sequences that can detect fresh thrombi and also measure the age of IPH lesions. Second, because the patients included in this study had been selected as candidates for CEA based on the criteria of our institute,¹²